Contents

1 Time-Dependent Density Functional Theory in Atomic Collisions

H.J. Lüdde

1.1 Introduction

Scattering processes leading to excitation or fragmentation of atomic or molecular systems are a source of information on various physical effects associated with the mutual Coulomb interaction of such many-particle systems. This Chapter focusses on the discussion of a quantum mechanical system (the electrons of the target) influenced by a classical environment (the projectile) that provides the energy which disturbs the electronic system [1]. The classical environment can, for instance, be realized by an intense laser field or an ion beam which imposes its time-dependence on the electronic subsystem and defines a typical time scale for the scattering process – femtoseconds for an electronic system exposed to a laser beam and attoseconds for heavy-particle collisions.

From a theoretical point of view it is the time-dependent many-electron problem which has to be solved for different external potentials representing the interaction with the classical environment. In practice one often has to be content with a single-particle approximation providing effective single-particle equations that can be solved for any active electron at the prize, however, that the true two-particle character of the electron-electron interaction has to be neglected.

It is the power of Density Functional Theory (DFT) to provide a mathmatical framework that allows to *exactly* map the many-electron system onto a set of effective single-particle equations. This Chapter gives an outline of the basic concepts behind time-dependent DFT based on a series of review articles [2–4] which document the activity in this field. For a comprehensive introduction to stationary DFT the monograph of R. Dreizler and E.K.U. Gross is specially recommended [5].

Although there is hardly an alternative to time-dependent DFT for a theoretical investigation of systems with *many* active electrons it is not always clear how to extract observables of the system to establish contact with experimental results. The second part of this article addresses this problem and gives an idea of its complexity.

A few applications of DFT for typical collisional situations are summarized at the end of this Chapter. Atomic units are used.

1.2 Basic Concepts of Time-Dependent Density-Functional Theory

Starting point for the theoretical description of a non-relativistic electronic system is the time-dependent Schrödinger equation (TDSE)

$$\mathrm{i}\partial_t \Psi(t) = \hat{H}(t)\Psi(t)\,, \tag{1.1}$$

which determines the propagation in time of the N-particle system evolving from its initial state

$$\Psi(t_0) = \Psi_0\,. \tag{1.2}$$

Although $\Psi(t)$ fully describes the electronic system it is of course not observable. In a typical collision problem one usually measures probabilities of finding some of the electrons in a given state or at a certain place in configuration space. These *inclusive probabilities* [6] can be expressed in terms of the *q-particle density* [7]

$$\gamma^q(\boldsymbol{x}_1, \ldots \boldsymbol{x}_q, t) = \binom{N}{q} \int \mathrm{d}^4 x_{q+1} \ldots \mathrm{d}^4 x_N \, |\Psi(\boldsymbol{x}_1, \ldots \boldsymbol{x}_q, t)|^2\,, \tag{1.3}$$

where $\boldsymbol{x}_j = (\boldsymbol{r}, s)$ denotes coordinates and spin of the j-th electron and $\mathrm{d}^4 x_j$ indicates summation over spin and integration over space coordinates, respectively. With the definition (1.3) $\gamma^q \mathrm{d}^3 r_1 \ldots \mathrm{d}^3 r_q$ describes the inclusive probability of finding q electrons at given positions in configuration space, while the remaining $N - q$ electrons are not detected explicitly. As a special case one obtains for $q = 1$ the spin-free one-particle density

$$n(\boldsymbol{r}, t) = \sum_s \gamma^1(\boldsymbol{r}, s, t)\,, \tag{1.4}$$

which is the key for the understanding of DFT.

The total hamiltonian which enters the TDSE (1.1)

$$\hat{H}(t) = \hat{T} + \hat{W} + \hat{V}(t) \tag{1.5}$$

includes the kinetic energy, the mutual Coulomb repulsion between the electrons

$$\begin{aligned} \hat{T} &= \sum_{j=1}^{N} (-\frac{1}{2}\nabla_j^2) \\ \hat{W} &= \sum_{i<j=1}^{N} \frac{1}{|\boldsymbol{r}_i - \boldsymbol{r}_j|}\,, \end{aligned} \tag{1.6}$$

and the external potential

$$\hat{V}(t) = \sum_{j=1}^{N} v(\boldsymbol{r}_j, t)\,, \tag{1.7}$$

which characterizes the geometry as well as the explicit time-dependence of the particular quantum system. This decomposition of the hamiltonian into a universal, time-independent part (1.6) and a system-specific time-dependent external potential is a second important ingredience for the conceptual understanding of DFT.

Let us, thus, define a map $\mathcal{F} : v(\boldsymbol{r}, t) \to \Psi(t)$ by solving the TDSE for different external potentials but common initial state Ψ_0. As the one-particle density is uniquely determined by the time-dependent many-particle state $\Psi(t)$ this obviously defines a second map $\mathcal{G} : v(\boldsymbol{r}, t) \to n(\boldsymbol{r}, t)$. The foundation of DFT involves the proof, that the map $\mathcal{G}$ is invertible, i.e. $\Psi(t)$ can be obtained as a functional of the one-particle density $\Psi(t) = \mathcal{F}\mathcal{G}^{-1} n(\boldsymbol{r}, t)$. As a consequence any observable which can be written as an expectation value $\langle\Psi(t)|\hat{O}(t)|\Psi(t)\rangle$ of a hermitian operator would then be uniquely determined by $n(\boldsymbol{r}, t)$.

More precisely the conditions under which $\mathcal{G}$ is a 1-1 map between the external potential and the one-particle density are formulated by the Runge-Gross theorem [8]:

- For every single-particle potential $v(\boldsymbol{r}, t)$ which can be expanded into a Taylor series with respect to time around $t = t_0$ there exists a map $\mathcal{G} : v(\boldsymbol{r}, t) \to n(\boldsymbol{r}, t)$ by solving the TDSE with a fixed initial state Ψ_0. This map can be inverted up to an additive merely time-dependent function in the potential.

At this point a few remarks might be appropriate: (i) As the invertibility of the map between potentials and densities can only be shown with respect to a given initial state Ψ_0, the solution of the TDSE rigorously depends on the density *and* the initial state. Consequently any observable of the system is a functional of n and Ψ_0. (ii) The potential as a functional of n is only determined up to a merely time-dependent function. This corresponds to an ambiguity in $\Psi(t)$ up to a time-dependent phase factor, which cancels out for any observable characterized by an operator that is free of time derivatives. (iii) The Runge-Gross theorem can be applied to any system characterized by a given interaction $\hat{W}$, in particular for $\hat{W} = 0$. This fact is used in the subsequent section where a set of effective one-particle Schrödinger equations yielding the *exact* one-particle density is derived.

1.3 Time-Dependent Kohn-Sham Equations

The gist of DFT is the determination of the exact one-particle density n from which any many-particle observable can be derived. Let us assume we

know this density and can calculate it from a set of N ficticious orbitals $\{\phi_j, j = 1, \ldots N\}$

$$n(\boldsymbol{r}, t) = \sum_{j=1}^{N} |\phi_j|^2 \,. \tag{1.8}$$

The ansatz (1.8) suggests that the orbitals fulfil a single-particle Schrödinger equation of the form

$$\mathrm{i}\partial_t \phi_j(\boldsymbol{r}, t) = \left(\frac{-\nabla^2}{2} + v_{\mathrm{KS}}(\boldsymbol{r}, t) \right) \phi_j(\boldsymbol{r}, t) \;, j = 1, \ldots N \,, \tag{1.9}$$

where the existence of the single-particle potential v_{KS} is assumed. (This is discussed in the literature under the topic *v-representability* [9]). If this potential exists the Runge-Gross theorem guarantees its uniqueness, i.e. there is up to an additive merely time-dependent function exactly one single-particle potential which together with the time-dependent Kohn-Sham (KS) equations (1.9) reproduces the *exact* one-particle density n. Essentially, the KS equations represent an exact mapping of the N-electron problem onto a set of N single-particle problems. The crucial point is, however, that one does not know the KS potential explicitly.

1.3.1 Kohn-Sham Potential

Nevertheless a few general properties of the KS potential can be established: (i) the KS potential is local in space in contrast to the exchange term in Hartree-Fock theory, (ii) by virtue of the Runge-Gross theorem the KS potential must be a unique functional of the exact density *for a given initial state* Ψ_0 and *for a given KS determinant* $\Phi_0 = \det(\phi_1, ..\phi_N)/\sqrt{N!}$. The latter condition can be largely simplified if we assume that the time-dependent electronic system evolves from a *non-degenerate ground state* of the initially undisturbed system which via stationary DFT is fully determined by its corresponding density $n_0(\boldsymbol{r})$. In this case the KS potential is a unique functional of the density alone

$$v_{\mathrm{KS}}[n, \Psi_0, \Phi_0] = v_{\mathrm{KS}}[n](\boldsymbol{r}, t) \,. \tag{1.10}$$

Based on the experience with single-particle pictures one usually splits the KS potential in its classical parts – the external (Coulomb) interaction $v(\boldsymbol{r}, t)$ and the Hartree potential v_{H} which includes the screening of the external potential due to the electrons – and a genuine quantum part v_{xc} the *exchange-correlation potential*

$$\begin{aligned} v_{\mathrm{KS}}[n](\boldsymbol{r}, t) &= v(\boldsymbol{r}, t) + v_{\mathrm{H}}[n](\boldsymbol{r}, t) + v_{\mathrm{xc}}[n](\boldsymbol{r}, t) \\ v_{\mathrm{H}}[n](\boldsymbol{r}, t) &= \int \mathrm{d}^3 r' \, \frac{n(\boldsymbol{r}', t)}{|\boldsymbol{r} - \boldsymbol{r}'|} \,. \end{aligned} \tag{1.11}$$

However, as nothing is known about the exchange-correlation potential so far, one needs an additional property of the many-particle system to determine the KS potential explicitly.

The solution of the TDSE corresponds to a stationary point of the action integral

$$\mathcal{A} = \int_{t_0}^{t_1} \mathrm{d}t \, \langle \Psi(t) | \mathrm{i}\partial_t - \hat{H}(t) | \Psi(t) \rangle \,, \tag{1.12}$$

which essentially should be a functional of n as Ψ is. The TDSE is then obtained by variation of $\mathcal{A}$ with respect to Ψ. Can one therefore conclude that the exact one-particle density is a stationary point of the action integral as well, thus $\delta\mathcal{A}/\delta n(\boldsymbol{r}, t) = 0$?

This is obviously not the case, as the Runge-Gross theorem predicts the functional $\Psi[n]$ only up to an arbitrary time phase. Because of the time-derivative in the Schrödinger operator $\mathrm{i}\partial_t - \hat{H}(t)$ the action (1.12) is in fact a functional of n *and* the undetermined phase (for a detailed discussion on appropriate action functionals see [4] and [10]). Consequently equation (1.12) is not useful as an additional source for the derivation of the KS potential.

A more pragmatic approach rests on the assumption that the time-dependence of the KS potential is only due to the time-dependence of the density, where the functional dependence on the density is taken from stationary DFT. This is called the *adiabatic* approximation. The exchange-correlation (xc) potential for a nondegenerate ground state is related to the corresponding energy on the basis of the Rayleigh-Ritz variational principle

$$\begin{aligned} v_{\mathrm{xc}}[n_0](\boldsymbol{r}) &= \frac{\delta E_{\mathrm{xc}}[n]}{\delta n(\boldsymbol{r})}|_{n(\boldsymbol{r})=n_0} \\ E_{\mathrm{xc}} &= T - T_s + W - E_{\mathrm{H}} \,, \end{aligned} \tag{1.13}$$

where T and W are the expectation values of the interacting system, T_s denotes the kinetic energy, and E_{H} the Hartree energy of the KS system. The functional derivative (1.13) yields the functional dependence of the xc-potential on $n_0(\boldsymbol{r})$ for any particular approximation of the energy functional E_{xc}. Replacement of the ground state density by $n(\boldsymbol{r}, t)$ is the essential idea of the adiabatic approximation.

The Local-Density Approximation

The most convenient ansatz for the xc-energy is based on the assumption that the energy functional can be locally approximated by that of the homogeneous electron gas. This *local-density approximation* (LDA) yields for the exchange part a simple analytic expression

$$v_{\mathrm{x}}^{\mathrm{LDA}} = -\frac{1}{\pi}(3\pi^2 n(\boldsymbol{r}, t))^{1/3} \,, \tag{1.14}$$

while the correlation part is given in terms of a parametrisation [11]. The LDA (or ALDA for adiabatic LDA) should give reasonable results for systems in which the density is slowly varying both in space and time. However, it is important to notice that the exchange potential (1.14) decreases exponentially giving rise to an asymptotically incorrect compensation of the self-energy contained in the Hartree term. In atomic physics this can be cured by forcing the correct asymptotic decrease of the KS potential [12].

The Optimized-Potential Method

The problems associated with the self-energy effects can be solved more systematically on the basis of orbital dependent density functionals. As the KS orbitals are also functionals of n one can express the xc-potential as a functional of the KS orbitals. Using the chain rule for functional differentiation one obtains

$$\begin{aligned} v_{\mathrm{xc}}(\boldsymbol{r}) &= \frac{\delta E_{\mathrm{xc}}}{\delta n(\boldsymbol{r})} \\ &= \int \mathrm{d}^3 r' \, \frac{\delta v_{\mathrm{KS}}(\boldsymbol{r}')}{\delta n(\boldsymbol{r})} \int \mathrm{d}^3 r'' \, \sum_{k=1}^{N} \frac{\delta \phi_k^*(\boldsymbol{r}'')}{\delta v_{\mathrm{KS}}(\boldsymbol{r}')} \frac{\delta E_{\mathrm{xc}}[\boldsymbol{\phi}]}{\delta \phi_k^*(\boldsymbol{r}'')} + cc\,, \end{aligned} \tag{1.15}$$

with cc indicating the complex conjugate of the preceding expression. For the x-only term the exact energy functional is known

$$E_{\mathrm{x}} = -\frac{1}{2} \int \mathrm{d}^3 r \int \mathrm{d}^3 r' \sum_{k,l=1}^{N} \delta_{m_{s_k}, m_{s_l}} \frac{\phi_k^*(\boldsymbol{r}) \phi_l(\boldsymbol{r}) \; \phi_l^*(\boldsymbol{r}') \phi_k(\boldsymbol{r}')}{|\boldsymbol{r} - \boldsymbol{r}'|}\,, \tag{1.16}$$

which together with (1.15) yields an integral equation for the local exchange part of the KS potential. This scheme, originally introduced by Talman and Shadwick [13] as *optimized (effective) potential method* (OEP $\rightarrow$ OPM) has shown to be very successful in ground state DFT [14] as well as in time-dependent systems. The local character of the x-potential allows for a compensation of the self-energy not only for the occupied ground state orbitals – as it is the case in Hartree-Fock theory – but also for the virtual orbitals which is of particular interest in time-dependent systems. First attempts to include correlation [15] are very promising for ground state problems but are yet too complex for time-dependent systems.

1.3.2 Numerical Solution of the Kohn-Sham Equations

The numerical solution of the time-dependent KS equations (1.9) is quite involved. It is the long range of the Coulomb interaction which requires (i) stable algorithms as one has to propagate atomic systems over large time scales and (ii) high accuracy to adequately account for the enormeous delocalization of the electronic density. It is, thus, not surprising that the development

of appropriate numerical methods is well represented in the literature. Two reviews on time-dependent methods for quantum-dynamics [16] document the lively activity in this field over the last two decades. More recent developments of particular interest for ion-atom collisions include (i) lattice techniques discretising the TDSE in configuration space [17], momentum space [18] or a combination thereof based on FFT algorithms [19], (ii) expansion methods relying on single-center [20] or two-center [21] basis sets, (iii) the hidden crossing method [22] valid for adiabatic collisions, and with a broad spectrum of applications (iv) the classical trajectory Monte Carlo method [23] which simulates the electronic system in terms of a statistical ensemble of classical point charges.

A little different in its philosophy is the *Basis Generator Method* (BGM) [24] which allows to optimize the finite solution space in the sense that the individual basis functions dynamically adapt themselves to the momentary structure of the KS orbitals. In its present implementation [25] the BGM proves to be successful for collisions between ions and atoms [26], or ions and small molecules [27], and, very recently, for laser assisted atomic collisions [28].

1.4 Extraction of Observables

The solution of the KS equations (1.9) is the one-particle density which describes the time propagation of the dynamical system to its final state. As the many-particle wavefunction is a functional of n any observable of the system must be a functional of the one-particle density as well. This is, however, a critical point in the application of time-dependent DFT as the functional dependence on n is only known for a few observables.

1.4.1 Exact Functionals

One observable which is accessible in all kinds of atomic scattering systems irrespective of the complex individual collision processes involved is the energy-loss of the system

$$\mathcal{E}(t) - \mathcal{E}_0 = \int_{t_0}^{t} \dot{\mathcal{E}}(t')\,\mathrm{d}t' \,. \tag{1.17}$$

If one calculates the time-derivative of the total energy taking into account that only the external potential is explicitly time-dependent [4,29]

$$\begin{aligned} \dot{\mathcal{E}} = \frac{\mathrm{d}}{\mathrm{d}t}\langle\Psi|\hat{H}(t)|\Psi\rangle &= \langle\Psi|\frac{\partial\hat{H}}{\partial t} - \mathrm{i}[\hat{H},\hat{H}]|\Psi\rangle \\ = \langle\Psi|\frac{\partial}{\partial t}\hat{V}(t)|\Psi\rangle &= \int n(\boldsymbol{r},t)\dot{v}(\boldsymbol{r},t)\,\mathrm{d}^3r \,, \end{aligned} \tag{1.18}$$

one obtains the energy-loss as an explicit functional of the density

$$\mathcal{E}(t) - \mathcal{E}_0 = \int_{t_0}^{t} \int n(\boldsymbol{r}, t') \dot{v}(\boldsymbol{r}, t) \, \mathrm{d}^3 r \, \mathrm{d}t' \,. \tag{1.19}$$

For $t \to \infty$ the energy-loss depends on the control parameters of the scattering system: (i) (b, E) impact parameter and energy of the impinging ion or (ii) (I, ω) intensity and colour of the laser.

The expectation value of the total momentum of a dynamical system can either be written as a functional of the KS current

$$\begin{aligned} \mathcal{P}(t) &= \langle \Psi | \hat{P} | \Psi \rangle = \frac{1}{\mathrm{i}} \sum_{j=1}^{N} \langle \Psi | \nabla_j | \Psi \rangle \\ &= \frac{1}{2\mathrm{i}} \int (\nabla - \nabla') \, n(\boldsymbol{r}, \boldsymbol{r}', t)_{|\boldsymbol{r}=\boldsymbol{r}'} \, \mathrm{d}^3 r = \int \boldsymbol{j}(\boldsymbol{r}, t) \, \mathrm{d}^3 r \,, \end{aligned} \tag{1.20}$$

with

$$\boldsymbol{j}(\boldsymbol{r}, t) = \frac{1}{2\mathrm{i}} \sum_{j=1}^{N} \{ \phi_j^*(\boldsymbol{r}, t) \nabla \phi_j(\boldsymbol{r}, t) - \phi_j(\boldsymbol{r}, t) \nabla \phi_j^*(\boldsymbol{r}, t) \} \tag{1.21}$$

or with the aid of the continuity equation

$$\partial_t n(\boldsymbol{r}, t) = -\nabla \boldsymbol{j}(\boldsymbol{r}, t) \tag{1.22}$$

and Green's theorem as a functional of the time derivative of the KS density [4]

$$\mathcal{P}(t) = \int \boldsymbol{r} \dot{n}(\boldsymbol{r}, t) \, \mathrm{d}^3 r = - \int \boldsymbol{r} (\nabla \boldsymbol{j}(\boldsymbol{r}, t)) \, \mathrm{d}^3 r = \int \boldsymbol{j}(\boldsymbol{r}, t) \, \mathrm{d}^3 r \,. \tag{1.23}$$

In the case of a heavy-particle collision the longitudinal and transversal components of the total momentum are experimentally observable

$$\begin{aligned} \mathcal{P}_{\parallel}(t) &= \int z \dot{n}(\boldsymbol{r}, t) \, \mathrm{d}^3 r \\ \mathcal{P}_{\perp}(t) &= \int \sqrt{x^2 + y^2} \dot{n}(\boldsymbol{r}, t) \, \mathrm{d}^3 r \,, \end{aligned} \tag{1.24}$$

allowing the determination of the scattering angle (k_i denotes the momentum of the incoming projectile)

$$\tan \theta \approx \theta = \frac{\mathcal{P}_{\perp}}{\mathcal{P}_{\parallel} + k_i} \,, \tag{1.25}$$

if the Coulomb repulsion between the nuclei is negligible.

Another set of global observables of the scattering system that can be expressed as functionals of the density under certain conditions are *net-probabilities* corresponding to the average number of electrons in a final state. If for a heavy-ion collision the density

$$n(\boldsymbol{r}, t) = n_{\mathrm{T}}(\boldsymbol{r}, t) + n_{\mathrm{P}}(\boldsymbol{r}, t) + n_{\mathrm{I}}(\boldsymbol{r}, t) \tag{1.26}$$

can be split into finite regions around the target (T), the projectile (P), and an infinite complement (I) in such a way that the total volume (V=T+P+I) of the one-particle configuration space does not contain interference terms between these parts the particle number can be written as

$$\begin{aligned} N &= \int_{\mathrm{V}} n(\boldsymbol{r},t)\,\mathrm{d}^3r = \int_{\mathrm{T}} n(\boldsymbol{r},t)\,\mathrm{d}^3r + \int_{\mathrm{P}} n(\boldsymbol{r},t)\,\mathrm{d}^3r + \int_{\mathrm{I}} n(\boldsymbol{r},t)\,\mathrm{d}^3r \\ &= P_{\mathrm{T}}^{\mathrm{net}} + P_{\mathrm{P}}^{\mathrm{net}} + P_{\mathrm{I}}^{\mathrm{net}}\,. \end{aligned} \tag{1.27}$$

$P_{\mathrm{x}}^{\mathrm{net}}$ corresponds to the average number of electrons which can be detected within the subvolume x. For the case of an initially neutral target and bare projectile these particle numbers can be interpreted as *net-ionization*, *net-capture*, and *net-loss* if one defines the electron loss probability

$$P_{\mathrm{loss}}^{\mathrm{net}} = P_{\mathrm{P}}^{\mathrm{net}} + P_{\mathrm{I}}^{\mathrm{net}} = N - P_{\mathrm{T}}^{\mathrm{net}}\,. \tag{1.28}$$

which in this situation corresponds to the average charge of the target.

1.4.2 Approximate Functionals

The situation becomes more involved if one is interested in less global information about the scattering system. In equation (1.3) the q-particle density was introduced as a measure for the inclusive probability of finding q electrons at given positions in space while the remaining $N-q$ electrons are somewhere. Formally these q-particle densities are related

$$\gamma^q(\boldsymbol{x}_1,\ldots\boldsymbol{x}_q,t) = \frac{q+1}{N-q}\int \mathrm{d}^4x_{q+1}\,\gamma^{q+1}(\boldsymbol{x}_1,\ldots\boldsymbol{x}_{q+1},t)\,, \tag{1.29}$$

which can be readily seen inserting the definition (1.3). The q-particle densities are normalized

$$\int_{\mathrm{V}^q} \mathrm{d}^4x_1\ldots\mathrm{d}^4x_q\,\gamma^q(\boldsymbol{x}_1,\ldots\boldsymbol{x}_q,t) = \binom{N}{q}\,, \tag{1.30}$$

where V^q indicates that all q electron coordinates run over the entire volume V. If one splits the volume in which the many-particle state is analyzed into subvolumes – e.g. V=T+I for a two-electron system which can either be excited or ionized by a laser beam – the normalization integral yields [30]

$$\begin{aligned} 1 &= \int_{\mathrm{V}^2} \gamma^2 = \int_{\mathrm{T}^2} \gamma^2 + 2\int_{\mathrm{TI}} \gamma^2 + \int_{\mathrm{I}^2} \gamma^2 \\ &= P_{\mathrm{T}^2} + P_{\mathrm{TI}} + P_{\mathrm{I}^2}\,. \end{aligned} \tag{1.31}$$

The probabilities in this case correspond to the sum over elastic scattering, single and double excitation (P_{T^2}), single ionization with possible simultaneous excitation (P_{TI}), and double ionization (P_{P^2}), respectively. The extension

to the more involved situation of a heavy-particle collision with a N-electron target is straightforward

$$1 = \int_{\mathrm{V}^N} \gamma^N = \int_{(\mathrm{T+P+I})^N} \gamma^N = \sum_{\nu=0}^{N} \sum_{\mu=0}^{\nu} \binom{N}{\nu} \binom{\nu}{\mu} \int_{\mathrm{T}^{N-\nu}\mathrm{P}^{\nu-\mu}\mathrm{I}^{\mu}} \gamma^N \quad (1.32)$$

where the terms of the sum correspond to the probability of finding simultaneously $N-\nu$ electrons with the target, $\nu-\mu$ electrons with the projectile, and μ electrons ionized. It is interesting to notice that the integration over the inifinite volume I can always be reduced to an integration over T or T and P. This is demonstrated for the simplest case (1.31), where the single ionization probability can be expressed as

$$\begin{aligned} P_{\mathrm{TI}} &= 2\int_{\mathrm{TI}} \gamma^2 = 2\int_{\mathrm{T(V-T)}} \gamma^2 = \int_{\mathrm{T}} \gamma - 2\int_{\mathrm{T}^2} \gamma^2 \\ &= P_{\mathrm{T}}^{\mathrm{net}} - 2\int_{\mathrm{T}^2} \gamma^2 \,, \end{aligned} \quad (1.33)$$

using equation (1.29). Together with the knowledge of the initial state this type of probability allows to analyze the final charge state of the collision system. There is obviously a tremendous number of simultaneous processes that can be observed in a coincident experiment if N electrons become activated by an external time-dependent field (see the Appendix for a list of examples).

However, these inclusive probabilities depend on the q-particle density and there is not much known about the relation between the q-particle and one-particle density on a mathematically exact level. One, thus, has to evaluate these probabilities within the independent particle picture [6], where the q-particle density is represented by a $q \times q$ determinant of the one-particle density matrix. Although this approach corresponds to neglecting the correlation in the final state it presents a way to calculate *any* kind of inclusive probability [31]. Nevertheless it is this part of the theory which has to be developed in order to make the power of time-dependent DFT fully available for the discussion of collisional systems.

1.5 Applications

1.5.1 Many-Electron Atoms in Strong Laser Fields

Atoms in strong laser fields have received increasing attention with the advent of strong femtosecond lasers [32]. New phenomena have been investigated in connection with multiphoton ionization: above threshold ionization, the stabilization of atoms with high laser intensity and frequency and the formation of harmonic spectra.

The external potential (1.7) for an atom in a linear polarized laser puls with shape function $f(t)$ is

$$v(\boldsymbol{r},t) = -\frac{Q_t}{r} + E_0 f(t)\sin(\omega_0 t)z\,. \tag{1.34}$$

Solutions of the time-dependent KS equations (1.9) are compared within the ALDA and OPM approaches to the KS potential, where the numerical procedure relies on a finite difference method in cylindrical coordinates employing a Crank-Nicholson algorithm for the time integration [33]. Typical observables of the system are multiple ionization and the harmonic spectrum. The latter can be formulated as an *exact* functional of n by calculating the Fourier transform of the induced dipole moment

$$d(t) = \int zn(\boldsymbol{r},t)\,\mathrm{d}^3r\,. \tag{1.35}$$

Consequently comparison with experiment is very promising. Multiple ionization can however only be calculated within the x-only approach of the q-particle density which for an initial He ground state exposed to a laser pulse yields according to (1.31)

$$\begin{aligned} P_{\mathrm{I}} &= 2p(1-p) \\ P_{\mathrm{I}^2} &= (1-p)^2 \\ p &= \frac{1}{2}\int_{\mathrm{T}} n(\boldsymbol{r},t\to\infty)\,\mathrm{d}^3r\,. \end{aligned} \tag{1.36}$$

There is obviously a problem with the x-only approximation (1.36)

$$P_{\mathrm{I}} = 2\sqrt{P_{\mathrm{I}^2}}(1-\sqrt{P_{\mathrm{I}^2}})\,, \tag{1.37}$$

as the relation between P_{I} and P_{I^2} [30] always predicts a maximum of 0.5 for the single-ionization while double-ionization can become much larger.

As mentioned above this is so far the bottle-neck for applications based on time-dependent DFT: no matter how exact the density of the propagating system can be obtained [34] one depends upon approximate functionals for the evaluation of some of the observables.

1.5.2 Ion-Atom Collisions Involving Many Active Electrons

Modern experimental techniques like COLTRIMS (COLd Target Recoil Ion Momentum Spectroscopy) allow to investigate atomic collisions with high accuracy on a very detailed level. A considerable amount of theoretically unexplained experimental data have been collected over the past ten years [35]. In contrast to the experimental situation it was only very recently that a nonperturbative description of atomic collisions involving *many* active electrons became feasible (for a collection of references see [36]). With increasing number of electrons there is hardly an alternative to time-dependent DFT if one

is tackling the many-particle problem in a systematic way. In this context it appears to be useful to investigate the influence of different approximations of the exact KS hamiltonian on effects associated with the electronic interaction during the collision process.

For that purpose the KS potential (1.11) is rewritten

$$v_{\mathrm{KS}}[n](\boldsymbol{r},t) = v(\boldsymbol{r},t) + v_{\mathrm{ee}}[n](\boldsymbol{r},t)\,, \tag{1.38}$$

where v_{ee} which includes the Hartree- and xc-potentials is decomposed into

$$v_{\mathrm{ee}}[n](\boldsymbol{r},t) = v_{\mathrm{ee}}[n_0](\boldsymbol{r}) + \delta v_{\mathrm{ee}}[n](\boldsymbol{r},t) \tag{1.39}$$

a stationary part $v_{\mathrm{ee}}[n_0]$ including the potential of the undisturbed system and the response potential $\delta v_{\mathrm{ee}}[n]$ depending on the time-dependent density.

- Within the no-response approach $\delta v_{\mathrm{ee}} = 0$ one finds that the LDA approximation of the exchange potential notoriously overestimates the electron loss process (net-capture and ionization) (1.28), whereas the OPM exchange yields accurate results [26,37]. This corresponds to the fact that a correct prediction of the first ionization potential depends on the correct treatment of the exchange potential. The incorrect asymptotic behaviour of the LDA potential leads to additional artificial structures in the doubly differential cross section for inclusive single-electron emission [38].
- The inclusion of response effects becomes important with decreasing impact energy as the electrons have more time to adapt to the actual potential. In particular q-fold ionization is considerably reduced by response effects as the binding energies of the residual electrons are increased during the collision [39]. q-fold capture might be reduced by the fact that the projectile charge decreases due to consecutive electron transfer [40].

These issues are discussed in closer detail in Chapter 2 of this book. So far it is difficult to judge the importance of correlation effects for the dynamical calculation. It certainly seems to be more important to include correlation in the evaluation of observables which again requires the knowledge of the functional dependence of these observables on the one-particle density.

1.5.3 Fragmentation of Atomic Clusters in Collisions with Ions

The fragmentation of atomic clusters exposed to an external laser field or as a result of a heavy particle collision are studied within the non-adiabatic molecular dynamics formalism. The theory combines the time-dependent LDA approach to the electronic motion with a molecular dynamics description for the classical paths of the cluster fragments. The relevant KS equations are either solved on a grid (for a review see [41]) or in a finite basis expansion of the time-dependent KS orbitals [42]. The latter formalism has been successfully applied to collisions between ions and sodium clusters followed by electron transfer [43] and fragmentation processes [44].

1.6 Conclusion

For time-dependent systems with many active electrons DFT provides a realistic if not the only practicable approach to the quantum many-body problem. The basic theorems state that the many-particle TDSE can be mapped onto a set of single-particle equations from which the exact one-particle density can be calculated. Any observable of the system is in principle exactly related to the density in terms of density-functionals.

Approximations are, however, necessary due to the fact that (i) the single-particle (KS) potential including the many-electron effects is not known exactly and (ii) the functional dependence of the observables on the density can so far be formulated only for a few cases.

The structural simplicity of the time-dependent KS equations opens the room for many applications in atomic and molecular physics which require a microscopic quantum theory but are far too complex for traditional methods.

Acknowledgements The author gratefully acknowledges friendly and fruitful collaborations with Reiner Dreizler, Tom Kirchner, and Marko Horbatsch.

Appendix

A few examples of probabilities as functionals of the q-particle density are collected in this appendix.

- The q-fold ionization of a N-particle system exposed to a laser pulse is

$$P_{\mathrm{I}^q} = \binom{N}{q} \int_{\mathrm{T}^{\mathrm{N}-\mathrm{q}}\mathrm{I}^{\mathrm{q}}} \gamma^N = \sum_{\nu=0}^{q} (-1)^\nu \binom{N-q+\nu}{N-q} \int_{\mathrm{T}^{\mathrm{N}-\mathrm{q}+\nu}} \gamma^{N-q+\nu} \,. \tag{1.40}$$

- Contrary to the q-fold ionization one defines the *inclusive* q-fold ionization, the probability of finding *at least* q electrons emitted to the continuum

$$P_{\mathrm{I}^q\Sigma} = \binom{N}{q} \int_{\mathrm{V}^{\mathrm{N}-\mathrm{q}}\mathrm{I}^{\mathrm{q}}} \gamma^N = \sum_{\nu=0}^{q} (-1)^\nu \int_{\mathrm{T}^\nu} \gamma^\nu \,. \tag{1.41}$$

- The transferionization in a collision between a bare ion and an initially neutral target can be calculated using equation (1.32): k-fold capture in coincidence with l-fold ionization is thus

$$P_{\mathrm{P}^k\mathrm{I}^l} = \binom{N}{k+l}\binom{k+l}{l} \int_{\mathrm{T}^{\mathrm{N}-\mathrm{k}-\mathrm{l}}\mathrm{P}^{\mathrm{k}}\mathrm{I}^{\mathrm{l}}} \gamma^N = \tag{1.42}$$

$$\sum_{\nu=0}^{l}\sum_{\mu=0}^{\nu} (-1)^\nu \frac{(N-l+\nu)!}{\mu!(\nu-\mu)!k!(N-k-l)!} \int_{\mathrm{T}^{\mathrm{N}-\mathrm{k}-\mathrm{l}+\mu}\mathrm{P}^{\mathrm{k}+\nu-\mu}} \gamma^{N-l+\nu} \,.$$

- Neutralization of the projectile in collisions between He^+ and a neutral target ((N+1)-electron system):

$$P_{\mathrm{He}} = \int_{\mathrm{P}^2} \gamma^2 - 3\int_{\mathrm{P}^3} \gamma^3 + 6\int_{\mathrm{P}^4} \gamma^4 \mp \ldots \approx \int_{\mathrm{P}^2} \gamma^2 \,. \tag{1.43}$$

  The higher order terms correct the inclusive capture probability for the production of negative ions. These probabilities are, however small.
- Ionization of the projectile for the same scattering system:

$$P_{\mathrm{He}^{2+}} = 1 - \int_{\mathrm{P}} \gamma + \int_{\mathrm{P}^2} \gamma^2 - \int_{\mathrm{P}^3} \gamma^3 \pm \ldots \approx 1 - \int_{\mathrm{P}} \gamma + \int_{\mathrm{P}^2} \gamma^2 \,. \tag{1.44}$$

All these probabilities can only be evaluated explicitly within the independent particle picture, where the q-particle density is given in terms of the one-particle density matrix elements

$$\gamma^q(x_1, \ldots x_q) = \begin{vmatrix} \gamma(x_1,x_1) & \gamma(x_1,x_2) & \ldots & \gamma(x_1,x_q) \\ \vdots & \vdots & \vdots & \vdots \\ \gamma(x_q,x_1) & \gamma(x_q,x_2) & \ldots & \gamma(x_q,x_q) \end{vmatrix} \tag{1.45}$$

References

1. J.S. Briggs and J.M. Rost: Eur. Phys. J. D **10**, 311 (2000)
2. E.K.U. Gross, J.F. Dobson, and M. Petersilka: Density Functional Theory of Time-Dependent Phenomena. In: *Topics in Current Chemistry 181*, ed. by R.F. Nalewajski (Springer, Berlin Heidelberg New York 1996)
3. K. Burke and E.K.U. Gross: A Guided Tour of Time-Dependent Density Functional Theory. In: *Density Functionals: Theory and Applications, Proceedings of the tenth Chris Engelbrecht Summer School in Theoretical Physics* ed. by D. Joubert (Springer, Berlin Heidelberg New York 1997)
4. N.T. Maitra, K. Burke, H. Appel, E.K.U. Gross, and R. van Leeuwen: Ten Topical Questions in Time-Dependent Density Functional Theory. In: *Review in Modern Quantum Chemistry: A Celebration of the Contributions of R.G. Parr* ed. by K.D. Sen (World Scientific 2001)
5. R.M. Dreizler and E.K.U. Gross: *Density Functional Theory* (Springer, Berlin Heidelberg New York 1990)
6. H.J. Lüdde and R.M. Dreizler: J. Phys. B **18**, 107 (1985)
7. P.-O. Löwdin: Phys. Rev. **97**, 1474 (1955)
8. E. Runge and E.K.U. Gross: Phys. Rev. Lett. **52**, 997 (1984)
9. M. Levy: Phys. Rev. A **26**, 1200 (1982)
   E.H. Lieb: Density Functionals for Coulomb Systems In: *Density Functional Methods in Physics* ed. by R.M. Dreizler and J. da Providencia (Plenum New York 1985)
10. R. van Leeuwen: Int. J. Mod. Phys. B **15**, 1969 (2001)
11. S.H. Vosko, L. Wilk, and M. Nusair: Can. J. Phys. **58**, 1200 (1980)
    J.P. Perdew and Y. Wang: Phys. Rev. B **45**, 13244 (1992)

12. R. Latter: Phys. Rev. **99**, 510 (1955)
J.P. Perdew: Chem. Phys. Lett. **64**, 127 (1979)
J.P. Perdew and A. Zunger: Phys. Rev. B **23**, 5048 (1981)
13. J.D. Talman and W.F. Shadwick: Phys. Rev. A **14**, 36 (1976)
14. E. Engel and R.M. Dreizler: J. Comp. Chem. **20**, 31 (1999)
15. A. Facco Bonetti, E. Engel, R.N. Schmid, and R.M. Dreizler: Phys. Rev. Lett. **86**, 2241 (2001)
16. K.C. Kulander (editor): *Thematic Issue on Time-Dependent Methods for Quantum Dynamics* Comp. Phys. Com. **63**, No: 1-3 (1991)
T. Kirchner, H.J. Lüdde, O.J. Kroneisen, and R.M. Dreizler: Nucl. Instr. and Meth. B **154**, 46 (1999)
17. D.R. Schultz, M.R. Strayer, and J.C. Wells: Phys. Rev. Lett. **82**, 3976 (1999)
18. D.C. Ionescu and A. Belkacem: Physica Scripta **T80**, 128 (1999)
19. M. Chassid and M. Horbatsch: J. Phys. B **31**, 515 (1998); Phys. Rev. A **66**, 012714 (2002)
A. Kolakowska, M. Pindzola, F. Robicheaux, D.R. Schultz, and J.C. Wells: Phys. Rev. A **58**, 2872 (1998)
A. Kolakowska, M. Pindzola, and D.R. Schultz: Phys. Rev. A **59**, 3588 (1999)
20. B. Pons, Phys. Rev. A **63**, 012704 (2001); ibid **64**, 019904 (2001)
K. Sakimoto, J. Phys. B **33**, 5165 (2000)
A. Igarashi, S. Nakazaki, and A. Ohsaki: Phys. Rev. A **61**, 062712 (2000)
X.M. Tong, D. Kato, T. Watanabe, and S. Ohtani: Phys. Rev. A **62**, 052701 (2000)
21. J. Fu, M.J. Fitzpatrick, J.F. Reading, and R. Gayet: J. Phys. B **34**, 15 (2001)
E.Y. Sidky, C. Illescas, and C.D. Lin: Phys. Rev. Lett. **85**, 1634 (2000)
N. Toshima: Phys. Rev. A **59**, 1981 (1999)
22. E.A. Solov'ev: Sov. Phys. Usp. **32**, 228 (1989)
M. Pieksma and S.Y. Ovchinnikov: J. Phys. B **27**, 4573 (1994)
23. C.L. Cocke and R.E. Olson: Phys. Rep. **205**, 163 (1991)
M. Horbatsch: Phys. Rev. A **49**, 4556 (1994)
C. Illescas and A. Riera: Phys. Rev. A **60**, 4546 (1999)
24. H.J. Lüdde, A. Henne, T. Kirchner, and R.M. Dreizler: J. Phys. B **29**, 4423 (1996)
25. O.J. Kroneisen, H.J. Lüdde, T. Kirchner, and R.M. Dreizler: J. Phys. A **32**, 2141 (1999)
26. T. Kirchner, L. Gulyás, H.J. Lüdde, A. Henne, E. Engel, R.M. Dreizler: Phys. Rev. Lett. **79**, 1658 (1997)
27. O.J. Kroneisen, A. Achenbach, H.J. Lüdde, and R.M. Dreizler: Model Potential Approach to Collisions Between Ions and Molecular Hydrogen. In: *XXII International Conference on Photonic, Electronic, and Atomic Collisions. Abstracts of Contributed Papers* ed. by S. Datz, M.E. Bannister, H.F. Krause, L.H. Saddiq, D. Schultz, and C.R. Vane (Rinton Press Princeton 2001)
28. T. Kirchner: Phys. Rev. Lett. **89**, 093203 (2002)
29. P. Hessler, J. Park, and K. Burke: Phys. Rev. Lett. **82**, 378 (1999)
30. H.J. Lüdde and R.M. Dreizler: J. Phys. B **16**, 3973 (1983)
31. P. Kürpick, H.J. Lüdde, W.D. Sepp, and B. Fricke: Z. Phys. D **25**, 17 (1992)
H.J. Lüdde, A. Macias, F. Martin, A. Riera, and J.L. Sanz: J. Phys. B **28**, 4101 (1995)
32. W. Becker and M.V. Fedorov (editors): *Focus Issue on Laser-Induced Multiple Ionization* Optics Express. **8**, No. 7 (2001)

33. M. Petersilka and E.K.U. Gross: Laser Physics **9**, 105 (1999)
M. Lein, E.K.U. Gross, and V. Engel: Phys. Rev. Lett. **85**, 4707 (2000); J. Phys. B **33**, 433 (2000); Phys. Rev. A **64**, 023406 (2001)
M. Lein, V. Engel, and E.K.U. Gross: Optics Express **8**, 411 (2001)
34. D.G. Lappas and R. van Leeuwen: J. Phys. B **31**, L249 (1998)
35. J. Ullrich, R. Moshammer, R. Dörner, O. Jagutzki, V. Mergel, H. Schmidt-Böcking, and L. Spielberger: J. Phys. B **30**, 2917 (1997)
R. Dörner, V. Mergel, O. Jagutzki, L. Spielberger, J. Ullrich, R. Moshammer, and H. Schmidt-Böcking: Phys. Rep. **330**, 95 (2000)
36. H.J. Lüdde, T. Kirchner, and M. Horbatsch: In: Quantum Mechanical Treatment of Ion Collisions with Many-Electron Atoms. In: *XXII International Conference on Photonic, Electronic, and Atomic Collisions. Invited Papers* ed. by J. Burgdörfer, J. Cohen, S. Datz, and C.R. Vane (Rinton Press Princeton 2002), p.708
37. T. Kirchner, L. Gulyás, H.J. Lüdde, E. Engel, and R.M. Dreizler: Phys. Rev. A **58**, 2063 (1998)
38. L. Gulyás, T. Kirchner, T. Shirai, and M. Horbatsch: Phys. Rev. A **62**, 022702 (2000)
39. T. Kirchner, M. Horbatsch, H.J. Lüdde, and R.M. Dreizler: Phys. Rev. A **62**, 042704 (2000)
40. T. Kirchner, M. Horbatsch, and H.J. Lüdde: Phys. Rev. A **64**, 012711 (2001)
41. F. Calvayrac, P.G. Reinhard, E. Suraud, and C. Ullrich: Phys. Rep. A **337**, 493 (2000)
42. U. Saalmann and R. Schmidt: Z. Phys. D **38**, 153 (1996)
43. O. Knospe, J. Jellinek, U. Saalmann, and R. Schmidt: Eur. Phys. J. D **5**, 1 (1999); Phys. Rev. A **61**, 022715 (1999)
Z. Roller-Lutz, Y. Wang, H.O. Lutz, U. Saalmann, and R. Schmidt: Phys. Rev. A **59**, R2555 (1999)
44. U. Saalmann and R. Schmidt: Phys. Rev. Lett. **80**, 3213 (1998)
T. Kunert and R. Schmidt: Phys. Rev. Lett. **86**, 5258 (2001)

2 Electron Interaction Effects in Ion-Induced Rearrangement and Ionization Dynamics: A Theoretical Perspective

T. Kirchner

2.1 Introduction

A considerable fraction of recent work in atomic and molecular collision physics was motivated by the quest for a better understanding of electron interaction effects. Excitation, rearrangement, and fragmentation patterns mirror various facets of the mutual Coulomb repulsion and the indistinguishability of electrons and provide a wealth of information on the characteristics and peculiarities of interacting many-fermion systems.

Naturally, the many-electron quantum dynamics is most transparent and best understood in situations, in which descriptions in terms of only a few coupled states or amplitudes of perturbation expansions are appropriate. In ion–atom collisions, which are considered in this Chapter, these conditions are met either at low impact energies, where the dominant capture processes are caused by nonadiabatic couplings between quasimolecular states, or in fast collisions of weakly charged ions, in which rearrangement and ionization processes can be described in terms of first- and second-order Born amplitudes. Such situations and corresponding theoretical approaches are well documented in the literature [1,2], and will not be discussed here. Instead, the intermediate energy regime, in which the coupling of different reaction pathways calls for a nonperturbative solution of the Schrödinger equation is addressed.

This region poses high demands on the theoretical treatment even for one-electron scattering systems. Only recently has it become possible to implement approaches for the simultaneous calculation of accurate total cross sections for capture, ionization, and excitation processes, and for the calculation of differential electron emission patterns (cf. Sect. 1.3.2 and references cited therein). A few works were also concerned with the fully correlated description of two-electron systems [3,4], in particular, with the ionization of helium atoms by protons (p) and antiprotons ($\bar{p}$) [5–8], which is regarded as a prime example for the manifestation of electron correlation effects.

A simple estimate shows that such explicit many-electron calculations will be prohibitive for systems with more than two active electrons for some time to come [9]. The outstanding interpretation of the rich experimental data

accumulated in recent years [10], therefore, calls for simplified approaches to the many-body problem of atomic collision physics. A few of such models, namely, the *Forced Impulse Method* [5], the *Frozen Correlation Approximation* [11], and the *Independent Time Approximation* [9] include some aspects of the electron–electron interaction explicitly without being computationally as costly as fully correlated calculations. Up to now, however, no applications to systems with more than two active electrons have been reported, which indicates the still demanding nature of these methods.

One may thus conclude that the only practicable approach to treat true many-electron systems in atomic collisions is some kind of effective single-particle description, i.e., the solution of single-particle equations for all active electrons. The usefulness of such independent particle models (IPMs) has been demonstrated in several works, but also their limited validity has been emphasized [2]: By definition they are not suited to discuss electron correlation effects.

It is explained in Chapter 1 of this book how Density Functional Theory (DFT) puts these issues into perspective. The central theorems of DFT ensure the existence of an *exact* mapping of the true many-body problem to an effective single-particle description, thus providing a sound basis for the application of IPM-type approaches. Admittedly, the promise to solve the many-body problem exactly is neglected in practice, since the exact expressions for many important quantities are not known and have to be approximated, but DFT proved to be a powerful tool for the description and understanding of dynamic [12] and, of course, stationary [13] many-body quantum systems.

It is the purpose of this contribution to demonstrate the usefulness of DFT for ion–atom collisions at intermediate impact energies. The key concepts of the time-dependent version of DFT, which provide the basis of this discussion are summarized in Chapter 1 and will not be explained in detail here. Only a few remarks at the beginning of Sect. 2.2 are in order to keep the discussion self-contained for a reader who is familiar with the basic ideas of DFT. After that, some specific approximations are introduced, which are both necessary to make the numerical solution of the problem at hand feasible, and helpful to classify the role of electron interaction effects in the collision dynamics. Some results, which are selected from a series of recent papers [14–21] are discussed in Sect 2.3. Emphasis is given to the analysis of different facets of the electron–electron interaction, which can be identified from the comparison of theoretical results with experimental data. Some concluding remarks are provided in Sect. 2.4.

2.2 Classification of Electron Interaction Effects: A Density Functional Approach

Ion–atom collisions at not too low impact energies can be discussed within the impact parameter model [22]: the motion of the nuclei is described in

terms of a classical straight-line trajectory $\boldsymbol{R}(t)$, which gives rise to a time-dependent external potential in the Hamiltonian (1.5) of the many-electron system (atomic units with $\hbar = m_e = e = 1$ are used)

$$\hat{V}(t) = \sum_{j=1}^{N} \left(-\frac{Z_\mathrm{T}}{r_j} - \frac{Z_\mathrm{P}}{|\boldsymbol{r}_j - \boldsymbol{R}(t)|} \right) . \tag{2.1}$$

Here, Z_T and Z_P denote the nuclear charges of the target and projectile nuclei, respectively, and $\boldsymbol{r}_j$ is the coordinate of the j-th electron. By virtue of the Runge-Gross theorem [23] the time-dependent many-electron problem can be mapped to an effective single-particle description, in which the *exact* density $n(\boldsymbol{r}, t)$ of the system is obtained from the solutions of single-particle equations (1.9). Moreover, the many-electron wave function as well as practically all observables of the system are uniquely determined by $n(\boldsymbol{r}, t)$. Hence, the so-called Kohn-Sham (KS) scheme is formally equivalent to solving the N-electron Schrödinger equation (1.1).

As discussed in Chapter 1 the downside of the structural simplicity of the KS scheme is the lack of knowledge of the true density dependences of the effective KS potential in the single-particle equations and of many important observables, such as multiple-ionization yields. Therefore, approximations are necessary on two fronts in practical calculations provided that the time-dependent KS equations can be solved accurately for a given potential. Such approximations and their physical implications are sketched in the next two Subsections.

2.2.1 Effects Associated with the Kohn-Sham Potential

Some general properties of the KS potential as well as the time-dependent *Local-Density Approximation* (LDA) and the time-dependent *Optimized-Potential Method* (OPM) are discussed in Sect. 1.3.1. These two approaches were used for the calculation of charge transfer in Ar^{8+}-Ar collisions [24], but results for ionization were not reported. Ionization has been considered very recently in $\bar{p}$-He collisions [25].

The work to be discussed in this Chapter relies on a decomposition of the KS potential into the external Coulomb potential of the projectile and target nuclei and two different contributions to the remaining effective electron–electron interaction v_ee: A stationary part v_ee^0 that accounts for the electron–electron interaction in the undisturbed ground state of the target atom, and a response potential δv_ee that depends on the time-dependent density and reflects the change of the electronic interaction in the presence of the projectile:

$$v_\mathrm{ee}(\boldsymbol{r}, t) = v_\mathrm{ee}^0(\boldsymbol{r}) + \delta v_\mathrm{ee}(\boldsymbol{r}, t) . \tag{2.2}$$

In the *no-response* approximation, δv_ee is neglected completely. This is well justified for fast collisions, in which the electronic density does not change

considerably during the short interaction time, and, more generally for one-electron transitions over a broad range of impact energies. One is then left with the question, which level of accuracy is needed for the ground-state potential v_{ee}^0 in order to obtain reliable results in these situations.

To investigate this issue, the effective potential v_{ee}^0 has been split into the classical Hartree and the exchange-correlation potentials, and two different approximations have been considered for the latter [14,15], which were tested extensively in atomic structure calculations [13,26]:

- the LDA [27], which similarly to the Hartree–Fock–Slater (HFS) approximation [28] rests on the density dependence of the homogeneous electron gas. As a consequence, the exchange part decreases exponentially in the asymptotic region rather than exhibiting the correct $-1/r$ tail. This deficiency is cured *a posteriori* by the Latter correction [30] or by more sophisticated self-interaction correction schemes [31], but exchange potentials of this type are, of course, only approximate. The smaller correlation contribution is given in terms of accurate analytic interpolation formulae [29].
- the OPM, in which exchange effects are treated nearly exactly [26,32]. It was also demonstrated that correlation can be included in the OPM in a systematic fashion [33], but test calculations with a semi-empirical correlation potential indicated that the static correlation contribution is too small to influence total scattering cross sections significantly [15].

From this short discussion it can be expected that the comparison of results obtained with the LDA and the OPM sheds light on the role of static exchange effects in collision processes. This is indeed the case and will be demonstrated in Sect. 2.3.1.

In the next step response effects have been included in the potential v_{ee} in a global fashion [18]. An important property of response is the increased attraction of the total target potential as soon as capture and ionization processes set in during the collision. This feature can be modeled by approximating the target potential as a linear combination of ionic ground-state potentials with time-dependent q-fold electron removal probabilities $P_q(t)$ as weighting factors. When the ionic potentials are related to the stationary potential v_{ee}^0 by simply adjusting the asymptotic tail of the latter one arrives at the target response potential [18]

$$\delta v_{ee}(r,t) = \frac{-1}{N-1} \sum_{q=1}^{N} (q-1) P_q(t) v_{ee}^0(r) \,. \tag{2.3}$$

The effects of target response on collision cross sections are discussed in Sect. 2.3.2. A similar model was devised to study projectile response effects which are associated with the unscreening of the projectile ion due to capture processes, but for the cases investigated so far projectile response turned out to be of minor importance [20].

A somewhat different response model was introduced recently to investigate $\bar{p}$-He collisions [21]. It is motivated by the fact that the no-response approximation predicts an instable quasimolecule ($\bar{p}$He) at internuclear distances $R \leq 0.5$ a.u., whereas the true adiabatic ground-state energy level lies below the threshold for single ionization for all R [34,35]. As a consequence, single ionization at low impact energies is too high when calculated in the no-response model.

In order to remedy this flaw an *adiabatic* response potential was constructed in [21] such that the binding energy of the lowest single-particle level reproduces the true ionization potential of the quasimolecule at small R. The potential was taken to be of the form

$$\delta v_{\mathrm{ee}}(\boldsymbol{r}, R) = -a(R)\mathrm{e}^{-r} - \frac{p(R) r \cos\theta}{[d(R)]^3 + r^3}\,, \tag{2.4}$$

with parameters $p(R)$, $d(R)$, and $a(R)$ adjusted to fulfill the condition mentioned above.

Such modeling of particular features of the electron–electron interaction poses the question of how to construct a response potential that comprises the desired properties automatically in a systematic fashion. The most promising approach is certainly the time-dependent OPM (Sect. 1.3.1). In the exchange-only limit the scheme has been worked out theoretically and has been applied to various physical problems, but a full implementation that allows the description of ionization and capture processes in ion–atom collisions has not been reported yet. A time-dependent correlation potential beyond the *adiabatic* approximation (Sect. 1.3.1) has only been proposed on the level of the LDA so far [36].

2.2.2 Effects Associated with the Density Dependence of Observables

In Sect. 1.4.1 it is explained how particle numbers for net ionization and net capture can be calculated exactly from the density at asymptotic times after the collision. Corresponding cross sections are well suited to study the effects associated with the KS potential, since they are not contaminated with approximations on the second front: the extraction of observables from the solutions of the KS equations.

The density dependence of more detailed observables, such as probabilities for finding q out of N electrons in the continuum is only known approximately. These probabilities can be expressed in terms of q-particle densities, which are given as $q \times q$ determinants of the one-particle density matrix in the exchange-only limit (cf. Sect. 1.4.2). The determinantal structure reflects the antisymmetry of the N-electron wave function, i.e., the Pauli principle is still taken into account on the level of the density matrix analysis.

Very often, the determinantal structure is neglected in practice, usually without analyzing this additional approximation. All probabilities of interest

can then be calculated by multinomial expressions of single-particle probabilities, which are sometimes modified to circumvent certain problems, such as non-zero probabilities for unphysical multiple-capture events [17]. It will be demonstrated in Sect. 2.3.3 for one obvious and one subtle example that the effects of the Pauli principle in the final states become apparent when data obtained from multinomial and density matrix analyses are compared.

In the case of a two-electron spin-singlet system evolving from its initial ground state the determinantal structure of the q-particle densities breaks down and the single- and double-ionization probabilities are reduced to the simple binomial formulae (1.36). That this exchange-only analysis is not compatible with double ionization probabilities obtained from more elaborate methods is pointed out in Sect. 2.3.4, in which some of the limitations of the present approach are sketched.

2.3 Identification of Electron Interaction Effects: Comparison with Experiment

As mentioned before, the accurate solution of the time-dependent KS equations for ion–atom collision systems is a delicate numerical problem even in the simplest case of the no-response approximation. Therefore, the developement of an efficient propagation method was a prerequisite for a meaningful investigation of electron interaction effects. The *Basis Generator Method* (BGM) [37] proved to be such a method in a number of succesful studies [14–21,38]. The idea of the BGM is the representation of the single-particle orbitals in a dynamically adapted model space, i.e., in terms of a basis that spans that part of the Hilbert space that is relevant for the specific problem under investigation.

Typically, the BGM basis sets used consist of undisturbed target eigenstates of the $1s$ through $4f$ states and a set of approximately 100 pseudo states generated by the repeated application of a regularized Coulomb potential at the projectile center on the undisturbed functions. The observables discussed below are extracted from the numerical solutions by the methods explained in Chapter 1.

2.3.1 Static Exchange Effects

The influence of static exchange effects on the ion–atom collision dynamics was studied by solving the time-dependent KS equations on the level of the no-response approximation with target ground-state potentials obtained from the OPM and the Latter-corrected LDA, respectively [14,15]. Let us focus on net ionization and capture cross sections at first in order to disentangle effects associated with the form of the KS potential from effects, which correspond to the approximate extraction of less global observables from the solutions of the KS equations.

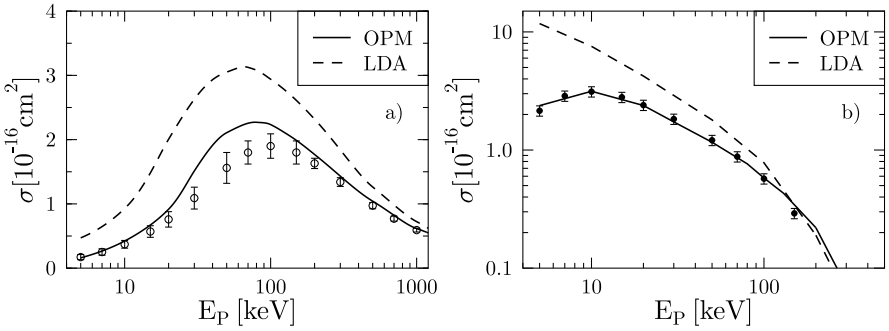

Fig. 2.1. (**a**) Net ionization and (**b**) net capture cross sections as functions of impact energy for p-Ne collisions. Lines: BGM calculations with different atomic potentials [48]. Experiment: open circles [49], closed circles [50]

In Fig. 2.1 results for the p-Ne collision system are presented. Clearly, the LDA leads to capture and ionization cross sections that are too large over the entire range of impact energies, whereas the agreement with the experimental data is convincing when the OPM potential is used. The failure of the LDA solutions can be traced back in part to the inaccurate prediction of the first ionization potential, i.e., to an underestimation of the binding energy of the outermost $2p$ electrons. However, it is not sufficient to correct this binding energy by simply adjusting the overall strength of the LDA exchange potential. This can be inferred from results for total [14] and differential [15,39] electron removal cross sections obtained with a HFS target potential whose exchange contribution differs from the LDA expression by the factor $\alpha = 3/2$. In particular, a thorough analysis of heavy-ion induced electron emission patterns demonstrated that the sudden switching from the exponentially decaying exchange potential to the asymptotic $-1/r$ tail introduced by the Latter correction is an additional source of errors and produces artificial structures in the doubly-differential cross section [39].

Two conclusions can be drawn at this point:

- Inaccurate treatments of the static exchange potential of the target atom lead to wrong electron removal cross sections. This demonstrates that static exchange effects are indeed mirrorred in such data.
- Response effects are of minor importance for proton induced transitions at least as long as net-electron processes are considered: Otherwise the results obtained with the OPM description of the target atom would not be in good agreement with the experimental data. Only at intermediate impact energies do we observe a theoretical net ionization cross section which lies above the experimental result [Fig. 2.1(a)]. From the discussion in the next Subsection it will become clear that this discrepancy is a signature of target-response effects.

2.3.2 Response Effects

Multiply charged projectile ions induce multiple-electron removal processes with higher probabilities than singly charged ions. They produce higher average recoil-ion charge states and should thus be more sensitive to response effects. Therefore, let us consider the He^{2+}-Ne collision system as a first application for the target response model (2.3) based on the static OPM potential.

As expected, the results for net ionization and capture (Fig. 2.2) obtained from the no-response approximation deviate more strongly from the experimental data than in the case of proton impact. Both cross sections are reduced at low and intermediate impact energies E_P when target response is included, while they are insensitive to response effects at higher E_P. This behavior confirms the earlier assumption that response is not effective when the projectile moves considerably faster than the outershell target electrons. In the case of ionization [Fig. 2.2(a)] the reduction of the cross section below $E_P = 500$ keV/amu leads to an almost perfect agreement of the target response data with the experimental results of [40]. These measurements are believed to be more accurate than the earlier data of [41] that are also included in the Figure.

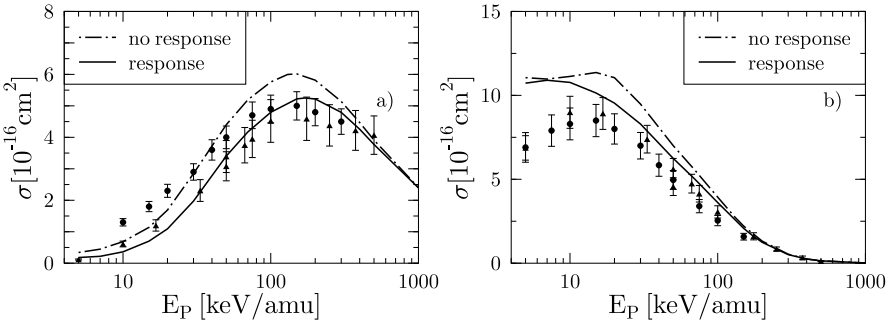

Fig. 2.2. (**a**) Net ionization and (**b**) net capture cross sections as functions of impact energy for He^{2+}-Ne collisions. Full and dash-dotted lines: BGM calculations with and without target response, respectively [18]. Experiment: closed triangles [40], closed circles [41]

For the capture channel [Fig. 2.2(b)], however, the agreement holds only down to $E_P = 20$ keV/amu, while the theoretical cross section lies above the experimental one at slower collisions. In this region, the influence of the response potential (2.3) on the capture cross section is rather small. This is partly due to a compensation of the behavior of electrons of different subshells: while capture of the $2s$ electrons is reduced by response effects the $2p$ electrons are transferred to the projectile with higher probability when δv_{ee} is included in the description. This is a consequence of the changing energy differences and coupling strengths between the relevant channels when

response is or is not taken into account. It suggests that the electron dynamics in slow collisions are rather sensitive to the specific form of the response potential. First attempts to include a spherical model for time-dependent projectile screening did not improve considerably upon the data of Fig. 2.2(b). At present, it is not clear whether a *microscopic* exchange-only response model, e.g., based on the time-dependent OPM would resolve the discrepancy with the experimental data or whether correlation plays a crucial role for electron capture in this energy region.

As a further example, the net ionization cross section for *singly* charged He-ion impact on Ne atoms is shown in Fig. 2.3. In this case, free electrons are produced by target and by projectile ionization, so that the time evolution of the active projectile electron driven by the target potential has also to be taken into account. This was done on the level of the no-response approximation by an analogous BGM expansion (details are discussed in [19]). It was found that 20–30 % of the cross section displayed in Fig. 2.3 stems from such projectile ionization events. The contribution due to target ionization is again reduced by target response, and the resulting net ionization cross section is in good agreement with the experimental data of [42]. Similar to the case of He^{2+}-impact these measurements are in conflict with earlier data obtained from a different experimental set-up [43], and are believed to be more accurate, although no clear explanation for possible errors in the earlier measurements was provided [42].

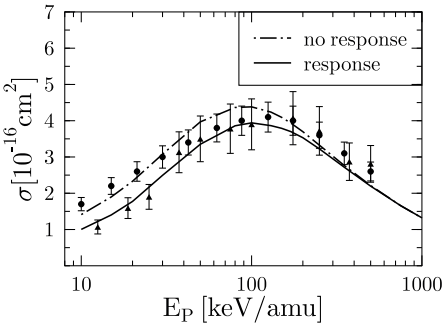

Fig. 2.3. Net ionization cross section as a function of impact energy for He^+-Ne collisions. Full and dash-dotted lines: BGM calculations with and without target response, respectively [19]. Experiment: closed triangles [42], closed circles [43]

Finally, results of the adiabatic response model for the ionization in $\bar{p}$-He collisions are discussed. In Fig. 2.4 the single ionization cross section obtained with and without adiabatic response is compared with experimental data and results of correlated two-electron calculations. Note that with the consideration of single instead of net ionization we are faced with the second source of errors besides the approximate form of the KS potential: we have to calculate the probability to remove *exactly* one electron from the target, which is only known in the exchange-only approximation (1.36). However, the effects of the exchange-only analysis should be of minor importance in

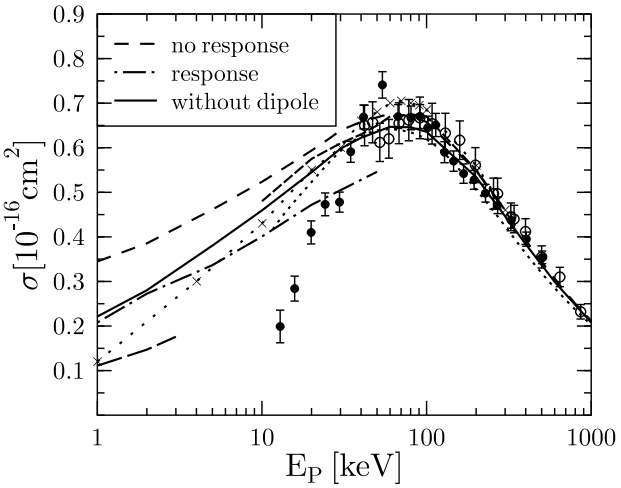

Fig. 2.4. Single ionization cross section as a function of impact energy for $\bar{p}$-He collisions. Theory: lines: BGM calculations with full adiabatic response, with adiabatic response without dipole contribution, and without response [21]; short-dashed curve [7], long-dashed curve [35], short-dotted curve, multi-cut FIM [5], long-dotted curve with crosses [6]. Experiment: closed circles [51], open circles [52]

the present case, in which multiple ionization events occur only with small probabilities and single ionization P_1 does not differ considerably from net ionization $P_{\mathrm{net}} = P_1 + 2P_2$. Evidently, such an argument does not apply when one considers double ionization (cf. Sect. 2.3.4).

Returning to the discussion of potential effects we first observe in Fig. 2.4 that there is a problem with the full adiabatic response potential of (2.4): The results lie considerably below the experimental and the other theoretical cross sections in the region above $E_P \approx 40$ keV, in which adiabatic effects should not play any role, as the electron cloud does not have enough time to adjust to the two-centre potential of the nuclei. When the calculations are repeated with the dipole contribution in (2.4) turned off the results do merge with the no-response cross section at intermediate impact energies. At lower E_P, however, they lie significantly below the no-response data, and are in close agreement with the cross section obtained with the full adiabatic response potential (2.4). Hence, the dipole part of (2.4) should be omitted entirely as it is relatively unimportant at low E_P and reduces the cross section wrongfully at higher E_P.

Remarkably, the results obtained with the dipole correction turned off are in good agreement with the much more elaborate two-electron calculations of [5–7] down to $E_P = 10$ keV. This demonstrates that the reduction of the no-response cross section in the 10 keV $\leq E_P \leq$ 50 keV range is not caused by explicit correlation effects, such as the deviation of the true two-electron wave function from a simple product form, but is mainly due to a

global response of the electron cloud in the presence of the antiproton. Note that this conclusion cannot be deduced from the results of the two-electron models, since it is difficult to trace different aspects of the electron–electron interaction in these 'complete' calculations.

At even lower impact energies the situation is less clear, since the coupled-channel calculation of [6] and the hidden-crossing calculation of [35] predict a significantly smaller cross section than the adiabatic response model, but are in conflict with each other. The picture becomes even more confusing when the experimental results are also taken into consideration as they lie below all theoretical data at $E_P \leq 30$–40 keV and do not seem to approach the results of the hidden-crossing calculation below 10 keV. New measurements are planned for the near future and may help to clarify this situation.

2.3.3 Pauli Blocking

In this Section effects associated with the antisymmetry of the final many-electron state are discussed. As mentioned in Sect. 2.2.2, the antisymmetry and the Pauli principle are maintained when the analysis is based on q-particle densities in the exchange-only approximation (cf. Sect. 1.4.2). By contrast, widely used multinomial formulae for q-particle probabilities rest on the assumption that the many-electron wave function can be expressed as a simple product state.

To demonstrate the role of the Pauli principle results for target electron capture and projectile electron loss in He^+-Ne collisions obtained from both types of analyses are presented in Fig. 2.5. More specifically, the multinomial results were calculated with the analysis in terms of products of binomials proposed in [17]. Standard multinomial statistics for capture suffers from the problem that one obtains non-zero probabilities for unphysical multiple capture events which correspond to the formation of negatively charged projectile ions. This problem is avoided in the products-of-binomials analysis. The unphysical channels are eliminated, and the net capture probability is distributed statistically over the physically allowed ones. All cross sections of Fig. 2.5 are extracted from the same set of single-particle calculations, which are based on the target-response model defined by (2.3) and the no-response approximation for the propagation of the active projectile electron [19].

The results for electron capture corresponding to the neutralization of the projectile ion [Fig. 2.5(a)] are easily explained. In the 'products' analysis both spin-up and spin-down electrons contribute to the cross section in the same fashion, since they are not hindered by the fact that the dominant final $He(1s^2)$ state is a spin-singlet. As a consequence, the experimental cross section is overestimated by almost a factor of two. The density matrix analysis, termed 'Pauli' in Fig. 2.5, takes this aspect into account and leads to nearly perfect agreement with experiment. Hence, the neutralization cross section reflects Pauli blocking very directly.

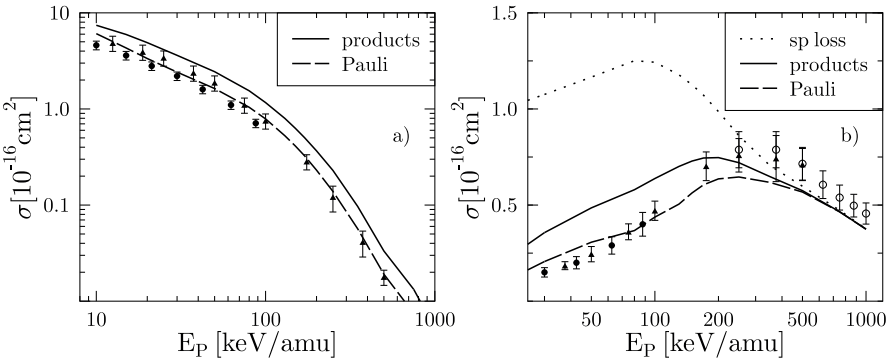

Fig. 2.5. Total cross sections for (**a**) neutralization of and (**b**) electron loss from the projectile as functions of impact energy for He^+-Ne collisions. Lines: BGM calculations with target response and final-state analysis in terms of products of binomials (full curve) and density matrix analysis (broken curve); The dotted curve in the right panel corresponds to a single-particle calculation for the active He^+ electron [19]. Experiment: closed triangles [42], closed circles [43], open circles [53]

The situation is more subtle for the case of projectile electron removal, for which the density matrix analysis reduces the cross section again by almost a factor of two from low to intermediate impact energies, and leads to very good agreement with experiment in this region [Fig. 2.5(b)]. At first sight, one might be surprised that the two analyses yield different results at all, since many configurations contribute to this process, and 'blocking' of final states should not be important. In fact, the observed reduction of the cross section in the density matrix analysis can only be understood with a formal argument based on probability conservation [19]: By incorporating the antisymmetry into the state vector the transferred electron density is redistributed such that the correct balance for He^0, He^+, and He^{2+} formation is obtained.

The redistribution is ineffective at high impact energies, where He^0 formation is very unlikely [cf. Fig. 2.5(a)]. In this region, the data obtained from both analyses merge, and are also in agreement with the result of a simple calculation with one active He^+ electron and frozen target electrons. All theoretical data lie somewhat below experiment in this region, which probably indicates the lack of a correlation contribution in the KS potential (cf. Sect. 2.3.4). The single-electron model overestimates the cross section badly at lower impact energies demonstrating that simultaneous electron transfer processes from the target to the projectile affect the final projectile charge state decisively and cannot be neglected.

Summarizing the discussion of this Section it can be stated that a careful analysis of the final wave function is crucial for the understanding of cross sections, for which the final charge state of the projectile (and of the target) are well-defined. The exchange-only analysis appears to be sufficient to explain the formation of He^0 and He^{2+} in He^+-Ne collisions quantitatively.

2.3.4 What Lies Beyond: Correlation Effects

All results presented in this Chapter have been obtained on the level of the exchange-only approximation. Correlation effects in the KS potential and in the analysis of the final wave function have been ignored. This Subsection has the purpose to exemplify the limitations of this treatment.

At first, we consider a case, for which correlation effects associated with the KS potential can be isolated. A critical look at the net ionization cross section in He^+-Ne collisions (Fig. 2.3) indicates that the theoretical results slightly underestimate the experimental data at impact energies above 200–300 keV/amu. Based on a perturbative description of the scattering process it was argued that ionization of the projectile electron, which contributes to net ionization can be induced either by an interaction with the (screened) target nucleus or by an interaction with one of the target electrons [2]. In particular, the second process, sometimes termed *antiscreening* has been the subject of many studies in recent years (see, e.g., [44,45] and references therein). When calculated in the plane-wave Born approximation and added to the theoretical net ionization cross section displayed in Fig. 2.3 it leads to an improved agreement with experiment [19].

From the DFT viewpoint antiscreening must be contained in the *exact* time-dependent KS potential, since the net ionization cross section is calculated from the density without approximation in the analysis. Furthermore, since the calculations displayed in Fig. 2.3 are based on the exchange-only OPM target potential and since response effects are unimportant at impact energies above 300 keV/amu we have strong reason to believe that it is the time-dependent correlation potential, which gives rise to the desired enhancement of the net ionization cross section. Its inclusion should also remove the more apparent discrepancies between the theoretical results and experiment in projectile ionization at high impact energies [Fig. 2.5(b)], for which the role of the antiscreening contribution is normally discussed rather than for net ionization [2,44]. Conceptually, however, this case is somewhat less clear, since the projectile electron loss cross section is not calculated exactly from the electron density, but in the exchange-only approximation, which might also influence the results.

The failure of the exchange-only *analysis* becomes apparent for the case of a two-electron system, for which it reduces to the simple binomial formulae (1.36) which predict a fixed relation between the one- and two-electron probabilities (1.37). This appears to be in conflict with the fact that the total single-ionization cross section is very similar in p- and $\bar{p}$-He collisions at high energies $E_P \geq 1$ MeV, while double ionization by antiprotons is significantly more efficient than by protons [46]. In principle, such a pattern is not prohibited by the exchange-only analysis as the impact parameter dependence of p- and $\bar{p}$-He ionization events could be such that an equal single-ionization and a different double-ionization cross section is obtained. However, this contradicts the expectation of perturbation theory, and in fact results of the

correlated Forced Impulse Method at $E_P = 2.31$ MeV [47] showed that the single-ionization probability is almost indistinguishable, while the double ionization probabilities exhibit pronounced deviations for p and $\bar{p}$ impact. The relation (1.37) is clearly violated.

This suggests that the important part of electron correlation in the regime of high impact energies is hidden in the unknown true density dependence of the double-ionization yield, and not in the KS potential. At lower E_P, dynamical effects should become more important, and both aspects of correlation might contribute to the fact that pronounced deviations from experiment and from correlated calculations occur when double ionization is calculated with the adiabatic response potential (2.4) and the binomial formulae (1.36) [21].

2.4 Concluding Remarks

It was the purpose of this Chapter to show that various facets of the many-electron dynamics in ion–atom collisions can be explained from the viewpoint of time-dependent Density Functional Theory. The effects of exchange and response contributions in the Kohn-Sham potential, and the role of Pauli blocking in the final states were analyzed by comparing calculations performed on different levels of approximation with experiment. This has only become possible with the developement of the Basis Generator Method for the accurate solution of the KS equations.

Given the reliability of the BGM and the accuracy of the experimental data remaining discrepancies can be attributed to *microscopic* response and correlation in the KS potential and correlation in the density dependence of the observables considered. In some cases, both aspects can be separated, which might be helpful for the developement of functionals that include correlations. Some ideas were reported for the case of the time-dependent KS potential in the literature, but – to the author's knowledge – no approaches for the calculation of observables, such as multiple-ionization yields beyond the exchange-only approximation have been developed so far. This would certainly be a major breakthrough for the application of DFT to ion–atom collisions, and, more generally, for the understanding of the time-dependent many-electron problem.

Acknowledgement I thank Hans Jürgen Lüdde and Marko Horbatsch for our fruitful and enjoyable collaboration.

References

1. R.Suzuki, A. Watanabe, H. Sato, J.P. Gu, G. Hirsch, R.J. Buenker, M. Kimura, and P.C. Stancil: Phys. Rev. A **63**, 042717 (2001)
2. J.H. McGuire: *Electron Correlation Dynamics in Atomic Collisions* (Cambridge University Press, Cambridge 1997)

3. C. Pfeiffer, N. Grün, and W. Scheid: J. Phys. B **32**, 53 (1999)
4. I.F. Barna: Ionization of helium in relativistic heavy-ion collisions. PhD Thesis, Universität Gießen, Germany (2002)
5. T. Bronk, J.F. Reading, and A.L. Ford: J. Phys. B **31**, 2477 (1998)
6. T.G. Lee, H.C. Tseng, and C.D. Lin: Phys. Rev. A **61**, 062713 (2000)
7. A. Igarashi, A. Ohsaki, and S. Nakazaki: Phys. Rev. A **62**, 052722 (2000); **64**, 042717 (2001)
8. C. Díaz, F. Martín, and A. Salin: J. Phys. B **35**, 2555 (2002)
9. A.L. Godunov and J.H. McGuire: J. Phys. B **34**, L223 (2001)
10. J. Ullrich, R. Moshammer, R. Dörner, O. Jagutzki, V. Mergel, H. Schmidt-Böcking, and L. Spielberger: J. Phys. B **30**, 2917 (1997)
    R. Dörner, V. Mergel, O. Jagutzki, L. Spielberger, J. Ullrich, R. Moshammer, and H. Schmidt-Böcking: Phys. Rep. **330**, 95 (2000)
11. C. Díaz, F. Martín, and A. Salin: J. Phys. B **33**, 4373 (2000)
12. N.T. Maitra, K. Burke, H. Appel, E.K.U. Gross, and R. van Leeuwen: Ten Topical Questions in Time-Dependent Density Functional Theory. In: *Review in Modern Quantum Chemistry: A Celebration of the Contributions of R.G. Parr* ed. by K.D. Sen (World Scientific 2001)
13. R.M. Dreizler and E.K.U. Gross: *Density Functional Theory* (Springer, Berlin, Heidelberg, New York 1990)
14. T. Kirchner, L. Gulyás, H.J. Lüdde, A. Henne, E. Engel, R.M. Dreizler: Phys. Rev. Lett. **79**, 1658 (1997)
15. T. Kirchner, L. Gulyás, H.J. Lüdde, E. Engel, and R.M. Dreizler: Phys. Rev. A **58**, 2063 (1998)
16. T. Kirchner, H.J. Lüdde, and R.M. Dreizler: Phys. Rev. A **61**, 012705 (2000)
17. T. Kirchner, H.J. Lüdde, M. Horbatsch, and R.M. Dreizler: Phys. Rev. A **61**, 052710 (2000)
18. T. Kirchner, M. Horbatsch, H.J. Lüdde, and R.M. Dreizler: Phys. Rev. A **62**, 042704 (2000)
19. T. Kirchner and M. Horbatsch: Phys. Rev. A **63**, 062718 (2001)
20. T. Kirchner, M. Horbatsch, and H.J. Lüdde: Phys. Rev. A **64**, 012711 (2001)
21. T. Kirchner, M. Horbatsch, E. Wagner, and H.J. Lüdde: J. Phys. B **35**, 925 (2002)
22. B.H. Bransden and M.R.C. McDowell: *Charge Exchange and the Theory of Ion-Atom Collisions* (Clarendon Press, Oxford 1992)
23. E. Runge and E.K.U. Gross: Phys. Rev. Lett. **52**, 997 (1984)
24. R. Nagano, K. Yabana, T. Tazawa and Y. Abe: J. Phys. B **32**, L65 (1999); Phys. Rev. A **62**, 062721 (2000)
25. X.M. Tong, T. Watanabe, D. Kato, and S. Ohtani: Phys. Rev. A **66**, 032709 (2002)
26. E. Engel and R.M. Dreizler: J. Comp. Chem. **20**, 31 (1999)
27. W. Kohn and L.J. Sham: Phys. Rev. **140**, A1133 (1965)
28. J.C. Slater: Phys. Rev. **81**, 385 (1951)
29. S.H. Vosko, L. Wilk, and M. Nusair: Can. J. Phys. **58**, 1200 (1980)
    J.P. Perdew and Y. Wang: Phys. Rev. B **45**, 13244 (1992)
30. R. Latter: Phys. Rev. **99**, 510 (1955)
31. J.P. Perdew and A. Zunger: Phys. Rev. B **23**, 5048 (1981)
32. J.D. Talman and W.F. Shadwick: Phys. Rev. A **14**, 36 (1976)
33. A. Facco Bonetti, E. Engel, R.N. Schmid, and R.M. Dreizler: Phys. Rev. Lett. **86**, 2241 (2001)

34. R. Ahlrichs, O. Dumbrajs, H. Pilkuhn, and H.G. Schlaile: Z. Phys. A **306**, 297 (1982)
35. G. Bent, P.S. Krstić, and D.R. Schultz: J. Chem. Phys. **108**, 1459 (1998)
36. J.F. Dobson, M.J. Bünner, and E.K.U. Gross: Phys. Rev. Lett. **79**, 1905 (1997)
37. H.J. Lüdde, A. Henne, T. Kirchner, and R.M. Dreizler: J. Phys. B **29**, 4423 (1996)
O.J. Kroneisen, H.J. Lüdde, T. Kirchner, and R.M. Dreizler: J. Phys. A **32**, 2141 (1999)
38. H.J. Lüdde, T. Kirchner, and M. Horbatsch: Quantum Mechanical Treatment of Ion Collisions with Many-Electron Atoms. In: *Photonic, Electronic, and Atomic Collisions* ed. by J. Burgdörfer, J. Cohen, S. Datz, and C.R. Vane (Rinton Press, Princeton 2002), p.708
39. L. Gulyás, T. Kirchner, T. Shirai, and M. Horbatsch: Phys. Rev. A **62**, 022702 (2000)
40. R.D. DuBois: Phys. Rev. A **36**, 2585 (1987)
41. M.E. Rudd, T.V. Goffe, and A. Itoh: Phys. Rev. A **32**, 2128 (1985)
42. R.D. DuBois: Phys. Rev. A **39**, 4440 (1989)
43. M.E. Rudd, T.V. Goffe, A. Itoh, and R.D. DuBois: Phys. Rev. A **32**, 829 (1985)
44. E.C. Montenegro, A.C.F. Santos, W.S. Melo, M.M. Sant'Anna, and G.M. Sigaud: Phys. Rev. Lett. **88**, 013201 (2002)
45. H. Kollmus, R. Moshammer, R.E. Olson, S. Hagmann, M. Schulz, and J. Ullrich: Phys. Rev. Lett. **88**, 103202 (2002)
46. H. Knudsen and J.F. Reading: Phys. Rep. **212**, 107 (1992)
47. A.L. Ford and J.F. Reading: J. Phys. B **23**, 2567 (1990)
48. T. Kirchner: Quantum-theoretical description of many-electron processes in ion–atom collisions. PhD Thesis, Universität Frankfurt a.M., Germany (1999)
49. M.E. Rudd, Y.K. Kim, D.H. Madison, and J.W. Gallagher: Rev. Mod. Phys. **57**, 965 (1985)
50. M.E. Rudd, R.D. DuBois, L.H. Toburen, C.A. Ratcliffe, and T.V. Goffe: Phys. Rev. A **28**, 3244 (1983)
51. P. Hvelplund, H. Knudsen, U. Mikkelsen, E. Morenzoni, S.P. Møller, E. Uggerhøj, and T. Worm: J. Phys. B **27**, 925 (1994)
52. L.H. Andersen, P. Hvelplund, H. Knudsen, S.P. Møller, J.O.P. Pederson, S. Tang-Pederson, E. Uggerhøj, K. Elsener, and E. Morenzoni: Phys. Rev. A **41**, 6536 (1990)
53. M.M. Sant'Anna, W.S. Melo, A.C.F. Santos, G.M. Sigaud, and E.C. Montenegro: Nucl. Instrum. Methods Phys. Res. B **99**, 46 (1995)